Biomaterials 29 (2008) 3743–3749

Contents lists available at ScienceDirect

Biomaterials

journal homepage: www.elsevier.com/locate/biomaterials

The control of cell adhesion and viability by zinc oxide nanorods

Jiyeon Lee [a], B.S. Kang [a], Barrett Hicks [a], Thomas F. Chancellor, Jr. [a], Byung Hwan Chu [a], Hung-Ta Wang [a], Benjamin G. Keselowsky [b], F. Ren [a], Tanmay P. Lele [a,*]

[a] Department of Chemical Engineering, University of Florida, Gainesville, FL 32611 6005, USA
[b] Pruitt Family Department of Biomedical Engineering, University of Florida, Gainesville, FL 32611, USA

ARTICLE INFO

Article history:
Received 29 March 2008
Accepted 23 May 2008
Available online 11 June 2008

Keywords:
Nanorods
Cell adhesion
Cell viability
Anti-adhesion

ABSTRACT

The ability to control the behavior of cells that interact with implanted biomaterials is desirable for the success of implanted devices such as biosensors or drug delivery devices. There is a need to develop materials that can limit the adhesion and viability of cells on implanted biomaterials. In this study, we investigated the use of zinc oxide (ZnO) nanorods for modulating the adhesion and viability of NIH 3T3 fibroblasts, umbilical vein endothelial cells, and capillary endothelial cells. Cells adhered far less to ZnO nanorods than the corresponding ZnO flat substrate. The few cells that adhered to ZnO nanorods were rounded and not viable compared to the flat ZnO substrate. Cells were unable to assemble focal adhesions and stress fibers on nanorods. Scanning electron microscopy indicated that cells were not able to assemble lamellipodia on nanorods. Time-lapse imaging revealed that cells that initially adhered to nanorods were not able to spread. This suggests that it is the lack of initial spreading, rather than long-term exposure to ZnO that causes cell death. We conclude that ZnO nanorods are potentially useful as an adhesion-resistant biomaterial capable of reducing viability in anchorage-dependent cells.

Published by Elsevier Ltd.

1. Introduction

The success of implanted devices such as orthopedic implants, cardiovascular prosthesis and neural electrodes is affected by the ability of cells to interact with the exposed device material. Because properties such as surface topology are stable features of the surface, compared to chemical modifications which may be degraded over time, there has been immense interest in directing cell behavior by controlling the topology of materials [1–16]. Cells have been found to respond differently to smooth surfaces compared to materials with micro- or nanoscale roughness in a cell type dependent manner [16–19].

Cells adhere to and spread on materials by assembling specialized supramolecular protein complexes called focal adhesions [20]. Focal adhesion assembly occurs through the ligation of integrin receptors to immobilized ligands such as fibronectin and subsequent clustering of ligated receptors. Variations in nanoscale topography of the substrate can modulate nanoscale integrin ligation and clustering, resulting in changes in adhesion assembly [18,21–23]. Because focal adhesions are signaling complexes [20], such changes in adhesion assembly can alter signaling pathways resulting in the regulation of cell behavior. Indeed, cell behaviors such as motility and adhesion, proliferation and differentiation have been found to be exquisitely sensitive to nanoscale topography of the substrate [1–18,22–24]. This sensitivity has been observed across a variety of cell types including fibroblasts, osteoblasts, endothelial, epithelial and smooth muscle cells [1–19,25,26]. At the nanoscale, cells have been found to be sensitive to a variety of surface topologies, which include nanopits [27], nanoposts [3], nanocracks [28], nanotubes [29] and nanoislands [4]. However, the mechanisms of cellular nano-sensing are not clear and are a subject of intense research [18,23].

One class of nanostructures that has received recent attention in the literature is a surface covered with upright slender cylinders, variously referred to as nanoposts, nanorods and nanocolumns [3–5,26,27]. A recent study showed that cell numbers and proliferation in fibroblasts are greatly reduced on needle-like silicon nanoposts [3]. This study suggests that nanoposts may be useful as anti-fouling materials. Such surfaces could potentially be used for modulating the fibrotic response around implanted biomaterials. However, another recent study showed that mesenchymal cells on Si nanowires survived for days, and even differentiated despite being impaled on Si nanowires [26,30]. Therefore, it is not clear if cells from different cell types will exhibit reduced cell survival on structures such as nanowires or nanorods.

In this paper, we developed a strategy to reduce cell adhesion and survival on surfaces by culturing cells of three different cell types on a monolayer of upright ZnO nanorods of 50 nm diameter and 500 nm height. A large number of nanorods were exposed to the cell (~60,000–150,000 per cell). Owing to the uniform

* Corresponding author. Tel.: +1 352 392 0317; fax: +1 352 392 9513.
E-mail address: tlele@che.ufl.edu (T.P. Lele).

0142-9612/$ – see front matter Published by Elsevier Ltd.
doi:10.1016/j.biomaterials.2008.05.029

distribution of the nanorod monolayer, the cells were not able to attach to any flat portion of the substrate. Our results indicate that initial adhesion, lamellipodia formation, dynamic cell spreading and cell survival at 24 h are greatly reduced on nanorod covered substrates in three different cell types. These results indicate the promise of using upright nanorod type structures for minimizing cell adhesion and survival.

2. Materials and methods

2.1. Fabrication of ZnO nanorods

ZnO nanorods were made by a solution-based hydrothermal growth method [31–33]. First, ZnO nanoparticles were prepared by mixing 10 mM zinc acetate dehydrate (Sigma Aldrich, St. Louis, MO) with 30 mM of NaOH (Sigma Aldrich, St. Louis, MO) at 58 °C for 2 h. Next, ZnO nanoparticles were spin-coated onto the substrate several times and then post-baked on a hot plate at 150 °C for better adhesion. The substrate with these 'seeds' was then suspended upside down in a Pyrex glass dish filled with an aqueous nutrient solution. The growth rate was approximately 1 μm/h with 100 ml aqueous solution containing 20 mM zinc nitrate hexahydrate and 20 mM hexamethylenetriamine (Sigma Aldrich, St. Louis, MO). To arrest the nanorod growth, the substrates were removed from solution, rinsed with de-ionized water and dried in air at room temperature.

2.2. Preparation of substrates for cell culture

For control substrate, we used 22 mm square glass cover slips (Corning, Inc., Lowell, MA) and ZnO flat substrates (Cermet, Inc., Atlanta, GA). Before use, each substrate was sterilized with UV for 5 min and cleaned in 70% ethanol and de-ionized water. After drying substrates in air at room temperature, they were treated with 5 μg/ml human fibronectin (FN) (BD biosciences, Bedford, MA). After overnight incubation with FN at 4 °C, the substrates were washed twice with PBS. Cell suspensions of the same concentration and volume (i.e. same number of cells) were then seeded on each substrate.

2.3. Cell culture and adhesion

Cells of three different types were seeded on FN-coated substrates. NIH 3T3 fibroblasts were cultured in DMEM (Mediatech, Inc., Herndon, VA) supplemented with 10% fetal bovine serum (FBS) (Hyclone, Logan, UT). Human umbilical cord vein endothelial cells (HUVECs) were cultured in EBM-2 Basal Medium and EGM-2 SingleQuot Kit (Lonza, Walkersville, MD). Bovine capillary endothelial cells (BCEs) were cultured in low-glucose DMEM supplemented with 10% fetal calf serum (FCS) (Hyclone, Logan, UT).

2.4. Immunostaining

After 24 h of cell seeding, non-adherent cells were removed with two gentle washes with PBS. The samples were fixed with 4% paraformaldehyde for 20 min and washed several times with PBS. Fixed cells were immuno-stained for vinculin and stained for actin using our previously reported methods [34,35]. Briefly, cells were fixed with 4% paraformaldehyde, permeabilized with 0.2% Triton X-100, and treated with mouse monoclonal anti-vinculin antibody (Sigma Aldrich, St. Louis, MO), followed by goat anti-mouse secondary antibody conjugated with Alexa Fluor 488 (Invitrogen, Eugene, OR). Actin was stained with phalloidin conjugated with Alexa Fluor 594 (Invitrogen, Eugene, OR). Cells were then imaged on a Nikon TE 2000 epifluorescence microscope using FITC and Texas Red filters. All images were collected using the NIS-Elements program (Nikon).

2.5. Cell viability assay

The live/dead viability/cytotoxicity kit for mammalian cells (Invitrogen, Eugene, OR) was used for quantifying adherent cell viability on each substrate. Cells were incubated at 30–45 min with calcein AM (2 μM for fibroblast, 5 μM for endothelial cells) and ethidium homodimer-1 (EthD-1) (4 μM for fibroblast, 1.5 μM for endothelial cells) [36]. Next, epifluorescence images of five random fields were collected on a Nikon TE 2000 inverted microscope using a 10× lens. The average number of cells adherent on each substrate, the number of adherent live cells (stained green with calcein AM) and adherent dead cells (stained red with EthD-1) were quantified from these images using the NIS-Elements program (Nikon). The experimental data was pooled and used for statistical comparisons using Student's *T*-test.

2.6. Scanning electron microscopy (SEM)

Cells were prepared for SEM by fixation with 2% glutaraldehyde buffered in PBS and post-fixed in 1% osmium tetroxide. Samples were next dehydrated in graded ethanol concentrations. Critical point drying (CPD) was performed on a Bal-Tec 030 instrument (ICBR Electron Microscopy Core Lab, University of Florida) followed by e-beam metal deposition (Ti/Au, 10/50 Å). SEM was performed on a Hitachi S-4000 FE-SEM (ICBR Electron Microscopy Core Lab, University of Florida). Images of samples were taken at 1.8–8.0k× magnifications.

2.7. Time-lapse imaging

Cells which had been cultured as mentioned above were trypsinized and re-suspended in bicarbonate-free optically clear medium containing Hank's balanced salts (Sigma Aldrich, St. Louis, MO), L-glutamine (2.0 mM), HEPES (20.0 mM), MEM essential and non-essential amino acids (Sigma Aldrich, St. Louis, MO), and 10% FCS [34]. Cells were passed onto FN-coated glass or ZnO nanorods, and phase contrast imaging performed overnight for 10 h on the Nikon TE 2000 microscope. Images were collected every 1 min, using a 20× objective.

3. Results

3.1. Formation of uniform ZnO nanorod monolayers

Shown in Fig. 1A are SEM images of ⟨001⟩ vertically-aligned ZnO nanorod arrays. Such nanorods could be grown over areas on the order of 1 cm^2; thus ZnO nanorods could be grown in uniform monolayers over very long distances compared to cellular length scales. The nanorods were approximately 50 nm in diameter, 500 nm in height and the density of nanorods was approximately 126 rods/μm^2. Based on measured cell spreading areas, this number corresponds to approximately 60,000 nanorods per fibroblast and approximately 75,000–150,000 nanorods per endothelial cell.

Because of our focus on the effect of topology on cells, it was important to choose an appropriate control for statistically comparing effects of nanorods on cells. As the material itself can have effects on protein adsorption and cell adhesion, we chose a topologically smooth substrate made of ZnO – a thin film commercially available from Cermet, Inc. An AFM image of this substrate is shown in Fig. 1B. The flat substrate is smooth over long length scales, with an average roughness of 1.33 nm. Interestingly, similar results were obtained for glass (average roughness of 1.34 nm, not shown), which allowed us to compare the performance of the ZnO flat substrate and ZnO nanorods with glass, a well-established substrate for cell culture.

3.2. Decreased cell spreading and focal adhesion formation on ZnO nanorods

We next investigated the influence of ZnO nanorods on cell spreading. Cells *in vitro* spread by assembling focal adhesions and stress fibers. Fig. 2 shows fluorescence images of three different cell types – NIH 3T3s, HUVECs, and BCEs on glass, ZnO flat substrate, and ZnO nanorods. Cells on ZnO flat substrates and glass cover slips assembled clear focal adhesions and stress fibers. Focal adhesions and stress fibers were not visible in cells on nanorods. The average area of cell spreading was decreased significantly on nanorods compared with ZnO flat substrates (a reduction of 60–70%, Table 1). These trends were observed in each of the three cell types.

3.3. Decrease in cell number and viability on ZnO nanorods

The results of Kim et al. [26] suggest that mesenchymal stem cells can survive on silicon nanowires for several days. Cells in this work were only exposed to 20–30 nanowires per cell. To investigate if the confluent monolayer of ZnO nanorods supports cell survival, we quantified the total cell number, and fraction of live and dead cells in the adherent population at 24 h of culture. The total number of adherent cells and of adherent live cells at the end of 24 h was greatly decreased on nanorods compared to flat substrates (Fig. 3) Because cells were seeded at equal cell densities on the two substrate types, the ratio of the number of attached cells on the ZnO nanorods to that on flat ZnO substrates represents the effect of

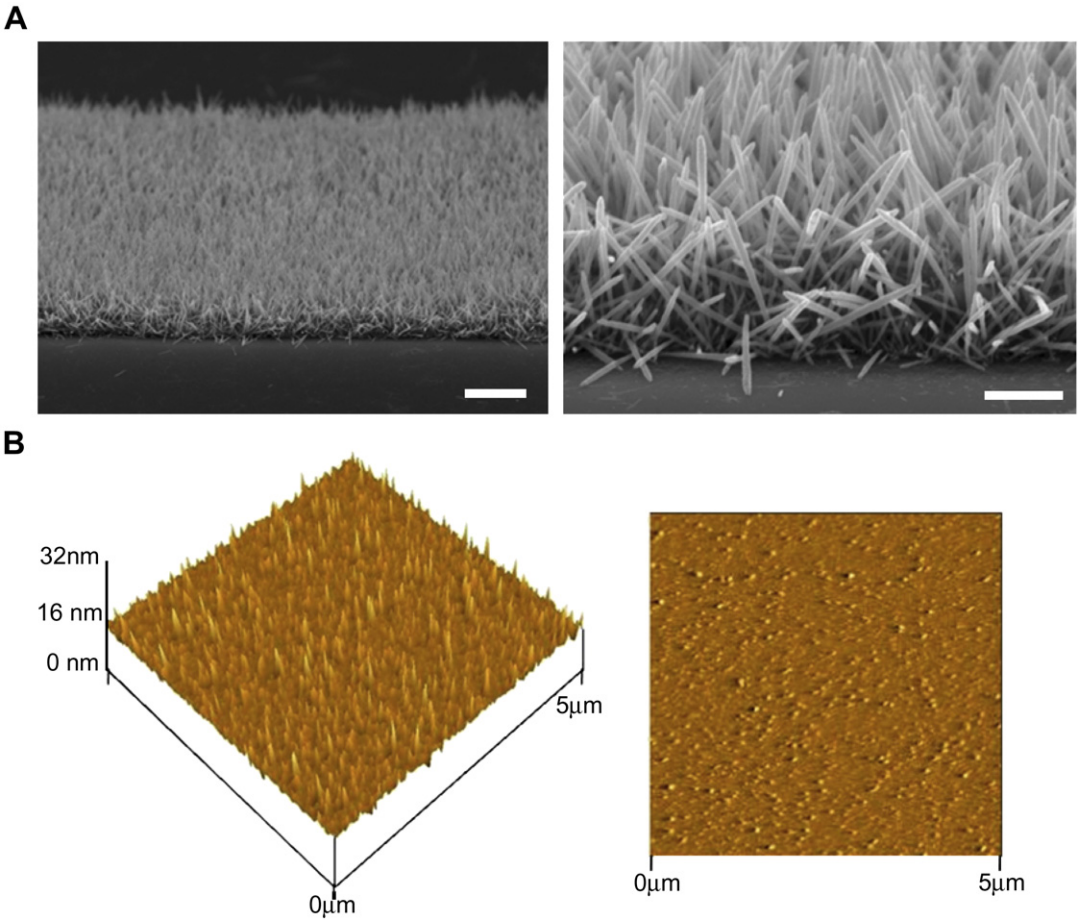

Fig. 1. The morphology of ZnO nanorods and flat substrate. (A) SEM images of ZnO nanorods indicating a uniform monolayer of ZnO (left, scale bar is 2 μm), and the upright growth of nanorods (right, scale bar is 500 nm). The diameter of nanorods was ~50 nm and the height was ~500 nm. (B) AFM image of ZnO flat substrate. The surface roughness was approximately 1.33 nm indicating that this substrate is much smoother than the nanorods and can be used for comparisons of cell behavior between nanorods and smooth surfaces.

topography (likely free from any other effects) on cell survival (Fig. 3D). The ratio of attached cells between ZnO nanorods and flat ZnO substrate is approximately same for all cell types. However, there was an order of magnitude decrease in cell survival in endothelial cells, and cell survival decreased by ~40% in fibroblasts (Fig. 3D). The fact that the fraction of attached live cells decreased on the nanorods in all three cell types is consistent with previous observations that topological cues at the nanoscale can profoundly modulate cell behavior [3,8,23].

3.4. Lack of lamellipodia and filopodia formation on ZnO nanorods

A recent study showed that cells on needle-like nanostructures only assemble filopodia [3]. To investigate this possibility for ZnO nanorods, we performed SEM studies on NIH 3T3 fibroblasts cultured on ZnO nanorods (Fig. 4). Most cells on ZnO nanorods were rounded (Fig. 4A). Instead of flat sheet-like lamellipodia, some cells formed thin processes (black arrow in Fig. 4B) and thin filopodia-like structures (white arrows in Fig. 4B) that appeared to attach to the ZnO nanorods. Therefore, while cells can attach to the ZnO nanorods using filopodia-like structures, they are not able to spread on the nanorods.

3.5. Decreased initial cell spreading on ZnO nanorods

In our studies, a large number of nanorods were exposed to cells. The results of Kim and co-workers showed that Si nanowires with diameter similar to our nanorods are engulfed by cells [26]. This raises the possibility that cells may spread initially on the nanorods but undergo apoptosis due to engulfment of nanorods at longer times. To clarify this, we performed time-lapse imaging for studying dynamic cell spreading on nanorods (Fig. 5). After seeding, initial adhesion of HUVECs on glass occurred in the first hour (Fig. 5A). Lamellipodia formation could be seen from 2 h onward followed by complete spreading at approximately 5 h (white arrows in Fig. 5A). Conversely, on nanorods, little initial spreading occurred and cells remained rounded over several hours (Fig. 5B). No lamellipodia formation was visible. These results show that nanorods did not support initial cell spreading. While these results alone do not rule out long-term toxicity of nanorods due to engulfment, they provide evidence that cells are not able to initially spread on nanorods, which may contribute to decreased survival at long times.

4. Discussion

ZnO nanorods, nanowires, and nanotubes have attracted considerable attention for biosensing applications owing to their chemical stability, high specific surface area, and electrochemical activity [37–39]. ZnO nanoplatforms have been developed for highly sensitive and specific detection of biological samples [40,41]. It is easy to control the aspect ratio and spacing of ZnO nanorods which is desirable for engineered materials [31]. However, before the promise of ZnO nanostructures for *in vivo*

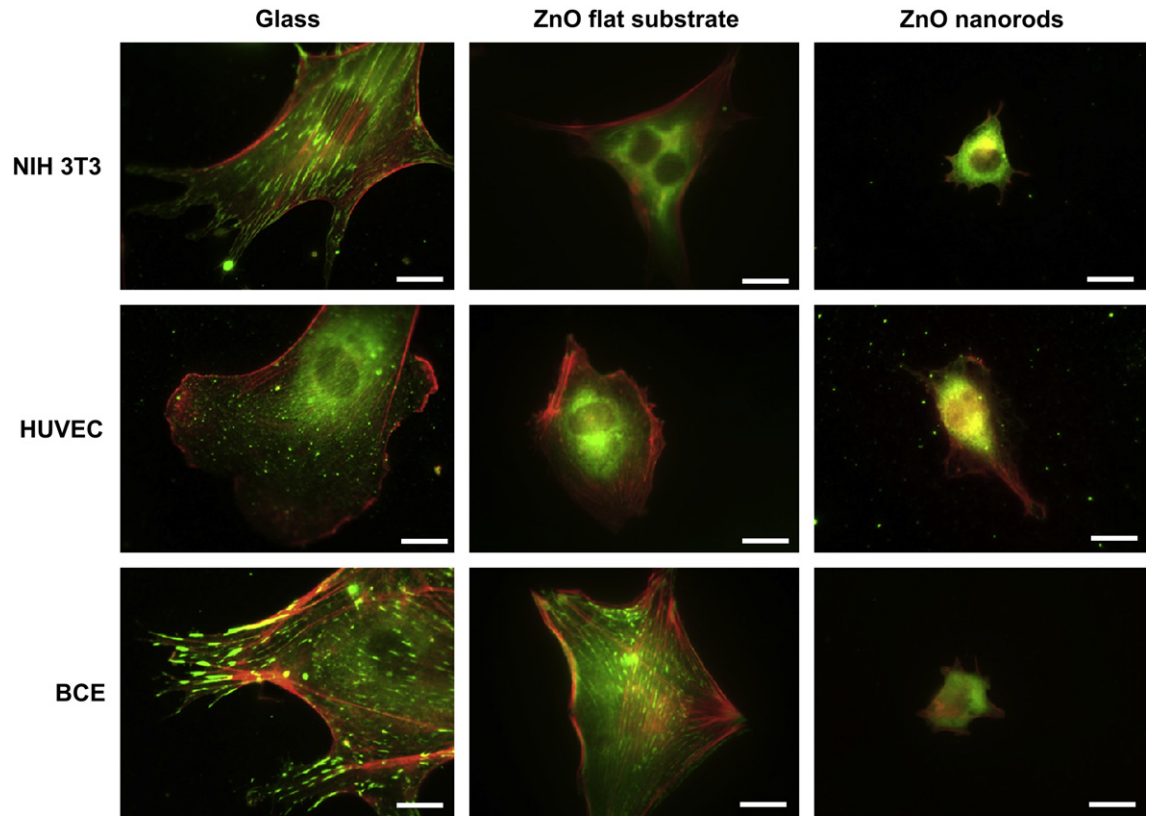

Fig. 2. Cells do not assemble stress fibers or focal adhesions on nanorods. Fluorescent micrographs of NIH 3T3, HUVEC, and BCE cells stained for vinculin (green) and F-actin (red) on glass, ZnO flat substrate and ZnO nanorods. The cell spreading area is greatly reduced, and focal adhesions and stress fibers are not visible in cells cultured on the nanorods. Scale bar is 20 μm.

applications can be realized, it is crucial to prevent cell adhesion to these structures.

In this paper, we found that the adhesion and viability of fibroblasts, umbilical vein endothelial cells, and capillary endothelial cells are greatly altered on ZnO nanorods. Cells adhered less and spread less on ZnO nanorods than the corresponding ZnO flat substrate. Scanning electron microscopy indicated that cells were not able to assemble lamellipodia on nanorods. Time-lapse phase contrast imaging showed that cells initially adherent to nanorods are unable to spread. This suggests that the lack of initial spreading on ZnO nanorods may cause cell death.

Our results indicate a lack of focal adhesion assembly in cells cultured on ZnO nanorods. The spacing between the ZnO nanorods is approximately 100 nm. Recent work by Arnold et al. showed that focal adhesion assembly requires that the spacing between ligated integrins be less than 70 nm [21]. Local integrin clustering probably can occur on single nanorods as their diameter is on the order of 50 nm. However, focal adhesions extend over several microns. It is possible that integrin clustering does not occur over contiguous lengths of micron length scales, preventing focal adhesion assembly. Cells on nanorods also have no visible lamellipodia. As initial adhesion is required to polymerize actin filaments [42], the lack of lamellipodia is probably due to an inability of cells to establish strong initial adhesion to the substrate, thereby altering the dynamics of cell spreading. Our observations of altered cell spreading dynamics are consistent with observations by Cavalcanti-Adam et al. who observed similar behavior on RGD (arginine–glycine–aspartic acid) nanopatterned substrates [22]. Our results can therefore be explained by a mechanism in which abnormal assembly of focal adhesions due to an inability to cluster integrins contributes to decreased cell spreading on nanorods. Because a lack of cell spreading can cause cell death in each of the cell types studied here [2,13], decreased spreading may explain the observed decrease in cell survival on nanorods.

It is interesting to contrast our results with the work of Kim et al. [26]. They found that nanowires are engulfed by cells, but do not induce apoptosis. Because the nanowires were sparse in this study (20–30 nanowires exposed to each cell), it is likely that cells attach to the flat portions of the substrate and therefore survived. In our experiments, each cell was exposed to ~60,000–150,000 nanorods. Thus, we cannot rule out the possibility that a large number of nanorods are engulfed by our cells. If this is the case, then toxicity due to nanorod engulfment may cause cell death. Indeed, phagocytosed ZnO nanoparticles have been reported to be cytotoxic in vascular endothelial cells [43]. More detailed studies are needed to investigate this possibility. If ZnO nanorods are engulfed by cells, then an interesting avenue for future investigation is the delivery of toxic material into cells. For example, the work by Kim et al. showed

Table 1
Average area of cell spreading on ZnO flat substrate and ZnO nanorods (average area ± standard error of the mean (μm^2))

	NIH 3T3	HUVEC	BCE
ZnO flat substrate	(1.44E+03) ± (2.76E+02)	(1.73E+03) ± (2.35E+02)	(4.18E+03) ± (7.49E+02)
ZnO nanorods	(4.73E+02) ± (7.44E+01)	(6.02E+02) ± (6.94E+01)	(1.22E+03) ± (1.17E+02)

The differences of cell spreading area on ZnO flat substrate *versus* ZnO nanorods were statistically significant ($n = 10$, for NIH 3T3 and BCE, $p < 0.005$ and for HUVEC $p < 0.0005$).

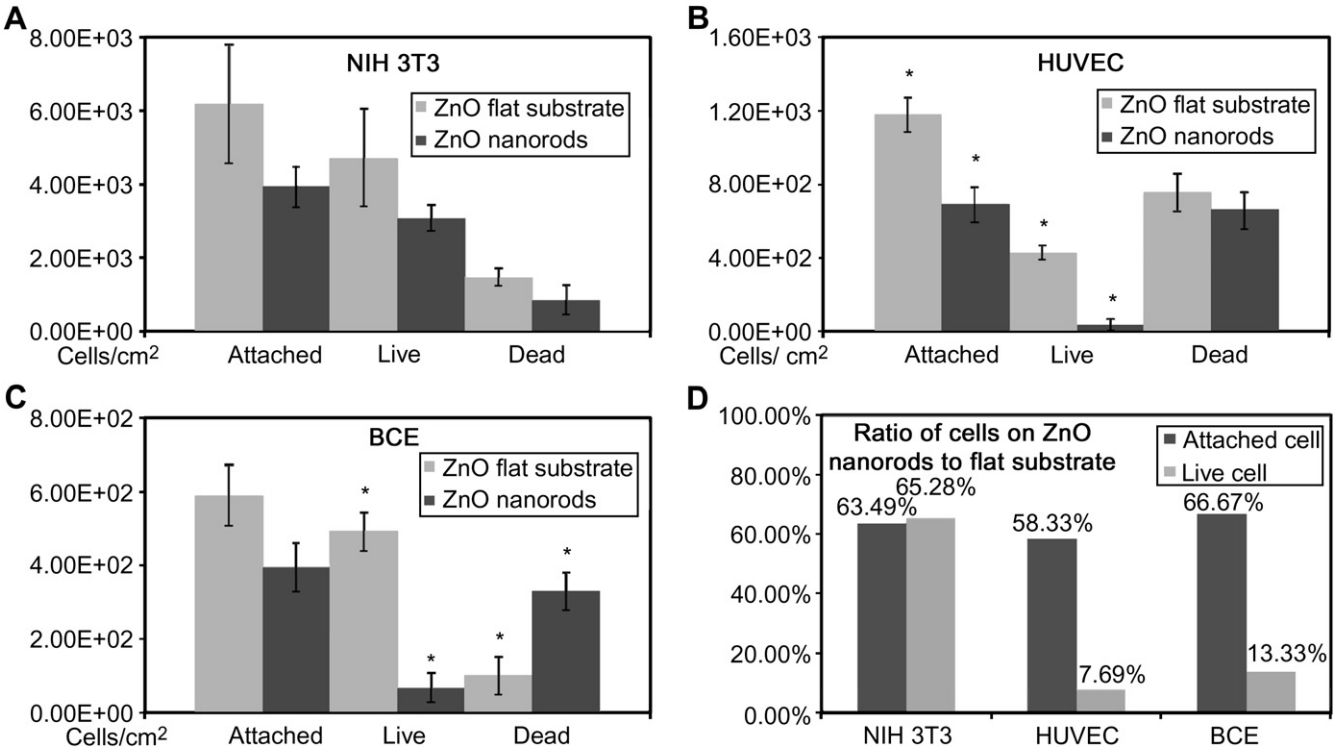

Fig. 3. Total cell number and number of live adherent cells are reduced on nanorods. The average number of cells adherent on each substrate, the number of adherent live cells (stained with calcein AM) and adherent dead cells (stained with EthD-1) were quantified in three cell types (A–C) by pooling data from five different images per cell type and condition. Bars indicate standard error of the mean. * Indicates statistically significant differences with $p < 0.01$ between the number of cells on ZnO nanorods and ZnO flat substrates ($n > 50$ for HUVEC, $n > 30$ for BCE, $n > 300$ for fibroblasts, where n is total number of cells). (D) The number of attached and live cells on ZnO nanorods is normalized by the number of attached and live cells on ZnO flat substrates, respectively. The results show that the ratio of attached cells on ZnO nanorods to that on ZnO flat substrates is approximately same for all three types of cells. The decrease in the number of live adherent cells on the nanorods is robust across three different cell types, with a larger effect demonstrated in endothelial cells (HUVEC, BCE) than fibroblasts (NIH 3T3).

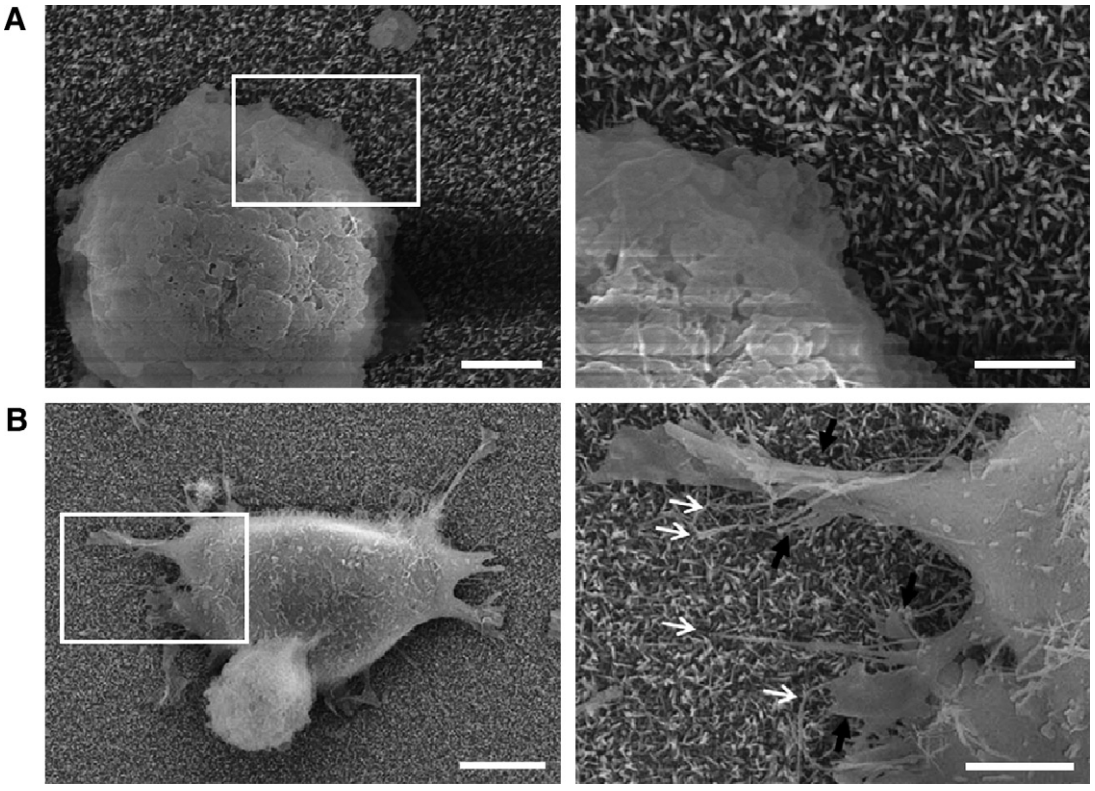

Fig. 4. Cells cannot assemble lamellipodia on nanorods. Representative SEM images of NIH 3T3 fibroblasts on ZnO nanorods. (A) Most of cells on ZnO nanorods were round and they did not form lamellipodia. Scale bars in left image and inset are 3 μm and 1 μm, respectively. (B) Filopodia-like structures were observed in some cells on nanorods (white arrows in inset) along with thin processes (black arrows). Scale bars in left image and inset are 5 μm and 2 μm, respectively.

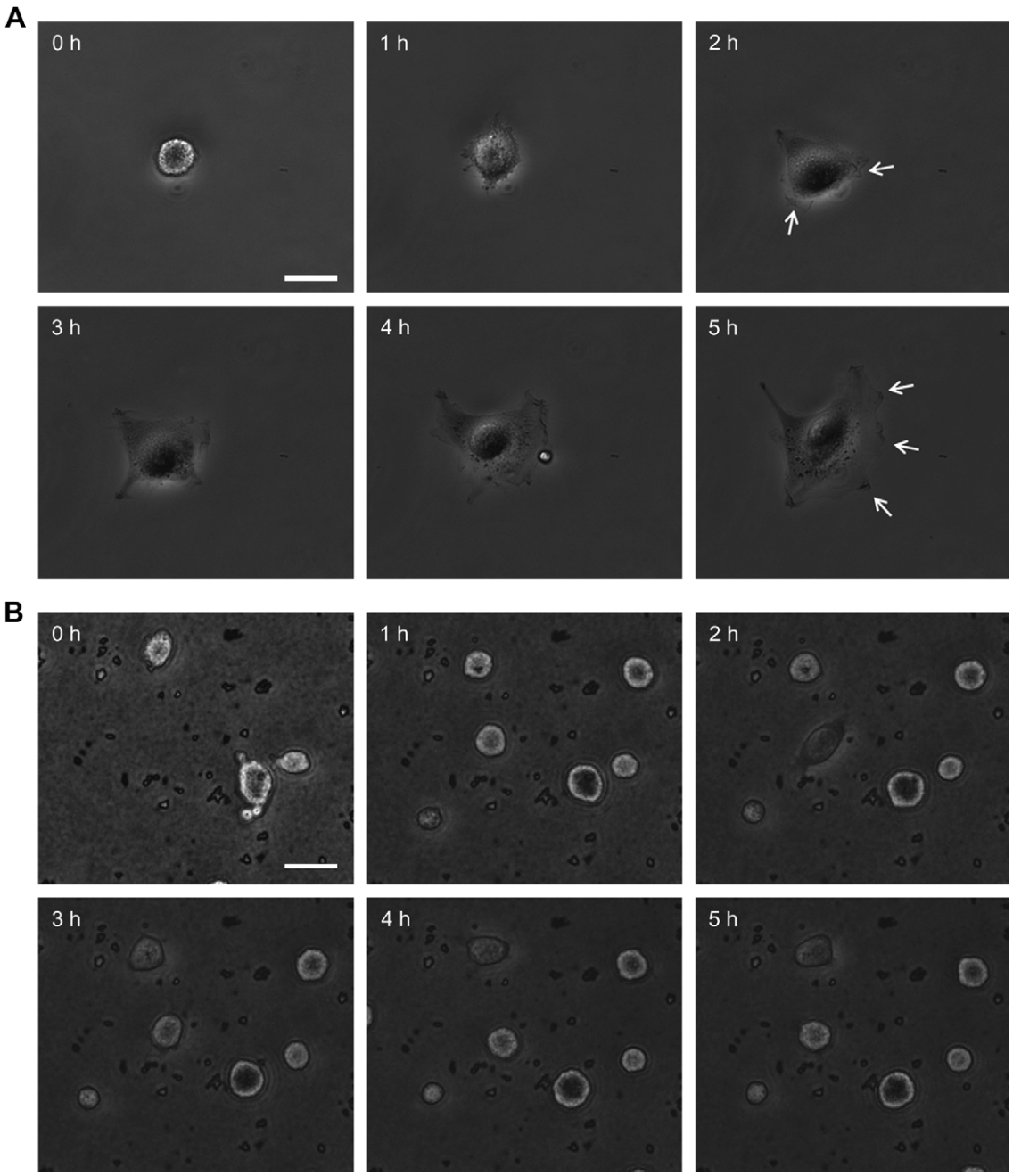

Fig. 5. Dynamic cell spreading is altered on nanorods. Phase contrast imaging of HUVECs spreading on glass and ZnO nanorods. (A) Cell spreading HUVECs is accompanied by lamellipodia formation (white arrows) and is complete in approximately 5 h. (B) Cells on nanorods do not spread, and do not develop any lamellipodia. Scale bar is 20 μm.

that DNA immobilized on Si nanowires could be delivered into cells [26]. Thus, the efficiency of ZnO nanorods in preventing cell survival may be further enhanced by chemically conjugating toxins to the surface, and delivering these into the cell through penetration and subsequent cleavage.

The nanorod aspect ratio probably plays an important role in the observed response. For example, Curtis and co-workers do not report a large decrease in cell survival, although they also observed decreased cell spreading on nanoposts [37]. The diameter in these studies was 100 nm and the height was 160 nm. Curtis et al. report that nanocolumns are not engulfed by cells. As our aspect ratio is more similar to Kim and co-workers [26] where the nanowires were engulfed by cells, this could be another reason for the decreased cell survival in our experiments. Additionally, our observations of reduced cell adhesion and survival on nanorods are consistent with at least one recent study which employed an aspect ratio similar to the one used in this paper [3].

5. Conclusions

Controlling cell behavior with biomaterials is necessary for the success of tissue engineering scaffolds, biomedical implants and implanted drug delivery devices. Collectively, our results indicate that ZnO nanorods can be used as an adhesion-resistant biomaterial capable of inducing death in anchorage-dependent cells. A better understanding of the mechanisms for the observed effects will be a key for designing optimal nanorod based substrates for minimizing cell adhesion and survival.

Acknowledgements

We are grateful to C. Sturm, K. Backer-Kelly, and K. Kelly for help in the SEM study. This work was partially supported by a grant from the American Heart Association (0735203N) to TPL.

References

[1] Andersson AS, Backhed F, von Euler A, Richter-Dahlfors A, Sutherland D, Kasemo B. Nanoscale features influence epithelial cell morphology and cytokine production. Biomaterials 2003;24:3427–36.
[2] Chen CS, Mrksich M, Huang S, Whitesides GM, Ingber DE. Geometric control of cell life and death. Science 1997;276:1425–8.
[3] Choi CH, Hagvall SH, Wu BM, Dunn JC, Beygui RE, Kim CJ. Cell interaction with three-dimensional sharp-tip nanotopography. Biomaterials 2007;28:1672–9.
[4] Dalby MJ, Riehle MO, Johnstone H, Affrossman S, Curtis AS. In vitro reaction of endothelial cells to polymer demixed nanotopography. Biomaterials 2002;23:2945–54.
[5] Dalby MJ, Riehle MO, Sutherland DS, Agheli H, Curtis AS. Morphological and microarray analysis of human fibroblasts cultured on nanocolumns produced by colloidal lithography. Eur Cell Mater 2005;9:1–8.
[6] Diehl KA, Foley JD, Nealey PF, Murphy CJ. Nanoscale topography modulates corneal epithelial cell migration. J Biomed Mater Res A 2005;75:603–11.
[7] Flemming RG, Murphy CJ, Abrams GA, Goodman SL, Nealey PF. Effects of synthetic micro- and nano-structured surfaces on cell behavior. Biomaterials 1999;20:573–88.
[8] Gonsalves KE, Halberstadt CR, Laurencin CT, Nair LS. Biomedical nanostructures. New York: John Wiley & Sons Inc.; 2007.
[9] Karuri NW, Liliensiek S, Teixeira AI, Abrams G, Campbell S, Nealey PF, et al. Biological length scale topography enhances cell-substratum adhesion of human corneal epithelial cells. J Cell Sci 2004;117:3153–64.
[10] Lenhert S, Meier MB, Meyer U, Chi LF, Wiesmann HP. Osteoblast alignment, elongation and migration on grooved polystyrene surfaces patterned by Langmuir–Blodgett lithography. Biomaterials 2005;26:563–70.
[11] Liliensiek SJ, Campbell S, Nealey PF, Murphy CJ. The scale of substratum topographic features modulates proliferation of corneal epithelial cells and corneal fibroblasts. J Biomed Mater Res A 2006;79A:185–92.
[12] Ma ZW, He W, Yong T, Ramakrishna S. Grafting of gelatin on electrospun poly(caprolactone) nanofibers to improve endothelial cell spreading and proliferation and to control cell orientation. Tissue Eng 2005;11:1149–58.
[13] Re F, Zanetti A, Sironi M, Polentarutti N, Lanfrancone L, Dejana E, et al. Inhibition of anchorage-dependent cell spreading triggers apoptosis in cultured human endothelial cells. J Cell Biol 1994;127:537–46.
[14] Teixeira AI, Abrams GA, Bertics PJ, Murphy CJ, Nealey PF. Epithelial contact guidance on well-defined micro- and nanostructured substrates. J Cell Sci 2003;116:1881–92.
[15] Teixeira AI, McKie GA, Foley JD, Bertics PJ, Nealey PF, Murphy CJ. The effect of environmental factors on the response of human corneal epithelial cells to nanoscale substrate topography. Biomaterials 2006;27:3945–54.
[16] Yim EKF, Reano RM, Pang SW, Yee AF, Chen CS, Leong KW. Nanopattern-induced changes in morphology and motility of smooth muscle cells. Biomaterials 2005;26:5405–13.
[17] Khang D, Lu J, Yao C, Haberstroh KM, Webster TJ. The role of nanometer and sub-micron surface features on vascular and bone cell adhesion on titanium. Biomaterials 2008;29:970–83.
[18] Spatz JP, Geiger B. Molecular engineering of cellular environments: cell adhesion to nano-digital surfaces. Methods Cell Biol 2007;83:89–111.
[19] Washburn NR, Yamada KM, Simon Jr CG, Kennedy SB, Amis EJ. High-throughput investigation of osteoblast response to polymer crystallinity: influence of nanometer-scale roughness on proliferation. Biomaterials 2004;25:1215–24.
[20] Bershadsky A, Kozlov M, Geiger B. Adhesion-mediated mechanosensitivity: a time to experiment, and a time to theorize. Curr Opin Cell Biol 2006;18:472–81.
[21] Arnold M, Cavalcanti-Adam EA, Glass R, Blummel J, Eck W, Kantlehner M, et al. Activation of integrin function by nanopatterned adhesive interfaces. Chemphyschem 2004;5:383–8.
[22] Cavalcanti-Adam EA, Volberg T, Micoulet A, Kessler H, Geiger B, Spatz JP. Cell spreading and focal adhesion dynamics are regulated by spacing of integrin ligands. Biophys J 2007;92:2964–74.
[23] Girard PP, Cavalcanti-Adam EA, Kemkemer R, Spatz JP. Cellular chemomechanics at interfaces: sensing, integration and response. Soft Matter 2007;3:307–26.
[24] Graeter SV, Huang J, Perschmann N, Lopez-Garcia M, Kessler H, Ding J, et al. Mimicking cellular environments by nanostructured soft interfaces. Nano Lett 2007;7:1413–8.
[25] Genove E, Shen C, Zhang SG, Semino CE. The effect of functionalized self-assembling peptide scaffolds on human aortic endothelial cell function. Biomaterials 2005;26:3341–51.
[26] Kim W, Ng JK, Kunitake ME, Conklin BR, Yang P. Interfacing silicon nanowires with mammalian cells. J Am Chem Soc 2007;129:7228–9.
[27] Dalby MJ, Gadegaard N, Wilkinson CDW. The response of fibroblasts to hexagonal nanotopography fabricated by electron beam lithography. J Biomed Mater Res A 2008;84A:973–9.
[28] Zhu XY, Mills KL, Peters PR, Bahng JH, Liu EH, Shim J, et al. Fabrication of reconfigurable protein matrices by cracking. Nat Mater 2005;4:403–6.
[29] Garibaldi S, Brunelli C, Bavastrello V, Ghigliotti G, Nicolini C. Carbon nanotube biocompatibility with cardiac muscle cells. Nanotechnology 2006;17:391–7.
[30] Pearton SJ, Lele T, Tseng Y, Ren F. Penetrating living cells using semiconductor nanowires. Trends Biotechnol 2007;25:481–2.
[31] Greene LE, Law M, Goldberger J, Kim F, Johnson JC, Zhang Y, et al. Low-temperature wafer-scale production of ZnO nanowire arrays. Angew Chem Int Ed Engl 2003;42:3031–4.
[32] Kang BS, Pearton SJ, Ren F. Low temperature (<100 degrees C) patterned growth of ZnO nanorod arrays on Si. Appl Phys Lett 2007;90:084104.
[33] Pacholski C, Kornowski A, Weller H. Self-assembly of ZnO: from nanodots, to nanorods. Angew Chem Int Ed Engl 2002;41:1188–91.
[34] Lele TP, Pendse J, Kumar S, Salanga M, Karavitis J, Ingber DE. Mechanical forces alter zyxin unbinding kinetics within focal adhesions of living cells. J Cell Physiol 2006;207:187–94.
[35] Parker KK, Brock AL, Brangwynne C, Mannix RJ, Wang N, Ostuni E, et al. Directional control of lamellipodia extension by constraining cell shape and orienting cell tractional forces. FASEB J 2002;16:1195–204.
[36] Michikawa M, Yanagisawa K. Apolipoprotein E4 induces neuronal cell death under conditions of suppressed de novo cholesterol synthesis. J Neurosci Res 1998;54:58–67.
[37] Al-Hilli SM, Willander M, Ost A, Stralfors P. ZnO nanorods as an intracellular sensor for pH measurements. J Appl Phys 2007;102:084304.
[38] Kang BS, Ren F, Heo YW, Tien LC, Norton DP, Pearton SJ. pH measurements with single ZnO nanorods integrated with a microchannel. Appl Phys Lett 2005;86:112105.
[39] Sun XW, Kwok HS. Optical properties of epitaxially grown zinc oxide films on sapphire by pulsed laser deposition. J Appl Phys 1999;86:408–11.
[40] Dorfman A, Kumar N, Hahm J. Nanoscale ZnO-enhanced fluorescence detection of protein interactions. Adv Mater 2006;18:2685–90.
[41] Dorfman A, Kumar N, Hahm JI. Highly sensitive biomolecular fluorescence detection using nanoscale ZnO platforms. Langmuir 2006;22:4890–5.
[42] Xia N, Thodeti CK, Hunt TP, Xu Q, Ho M, Whitesides GM, et al. Directional control of cell motility through focal adhesion positioning and spatial control of Rac activation. FASEB J 2008.
[43] Gojova A, Guo B, Kota RS, Rutledge JC, Kennedy IM, Barakat AI. Induction of inflammation in vascular endothelial cells by metal oxide nanoparticles: effect of particle composition. Environ Health Perspect 2007;115:403–9.